

## Formation of the light extracting surface of IR (850 nm) light-emitting diodes

© A.V. Malevskaya, N.A. Kalyuzhnyy, D.A. Malevskii, A.A. Blokhin, M.V. Nakhimovich, N.D. Il'inskaya

Ioffe Institute, St. Petersburg, Russia

E-mail: amalevskaya@mail.ioffe.ru

Received February 22, 2024

Revised April 5, 2024

Accepted April 10, 2024

Investigation of post-growth technology development of IR (850 nm) light-emitting diodes based on AlGaAs/GaAs heterostructures, grown by metalorganic vapour-phase epitaxy, has been carried out. Various methods of texturing and brightening the light extracting diode surfaces have been investigated, and a technology for forming optical elements has been developed. Analyzed was the relationship between chip formation technology and photovoltaic parameters of light-emitting diodes: electroluminescence intensity, optical power and external quantum efficiency. As a result of the developed technology, a twofold optical power value increase was achieved, which amounted  $> 400$  mW at current 800 mA.

**Keywords:** IR light-emitting diode, texturing, antireflection coating, optical element.

DOI: 10.61011/TP.2024.06.58825.47-24

### Introduction

Infrared (IR) light emitting diodes (LEDs) are widely used as emitters for optical sensors in wireless devices, in night vision systems, air drones et., [1,2]. Developments of new device designs for more effective output of the generated emission from a crystal are caused by rising requirements to the optical capacity of emitters. Development of heterostructures with multiple quantum wells (QWs), built-in structural reflectors based on the layers of a Bragg reflector, additional metal reflectors based on Ag or Au, providing for reflection of the emission spreading towards an absorbing substrate, makes it possible to achieve higher values of output capacity of LEDs [3–5].

Increased intensity of emission output is also achieved by optimization of technology for formation of the frontal light emitting surface of LEDs. The main methods include surface texturing, deposition of an antireflection coating and formation of an optical element (OE), as well as a combination of these methods. Formation of the textured developed light emitting area increases the surface area for the yield generated in the active emission area, and also changes the angle of reflection of incident photons, which increases the probability of their exit from the crystal at multiple reflection. Formation of the antireflection coating on the light emitting surface increases the share of the extracted emission. Packaging of LED crystals consists in formation of OE on the light emitting surface, which is made from material having optical transparency, with the refraction index value  $n$  between air and GaAs ( $1 < n < 3$ ), high stability and tightness. Use of OE material with the refraction index value lower than that of a semiconductor but higher than that of air, reduces the angle of full inner reflection and improves the extraction emission from the crystal [6].

This paper performed experimental research on optimization of technology for formation of the light emitting surface of LED crystals. New methods for surface texturing were developed, the compositions of the layers of antireflection coatings were optimized, and various OE designs were developed. Impact of various process approaches was analyzed at the evenness of the emission extraction, external quantum yield and optical capacity of IR LEDs.

### 1. Technology for formation of LED with built in metal reflector

IR LEDs with emission wave length of 850 nm were made on the basis of AlGaAs/GaAs-heterostructures with multiple QWs in the active area grown on GaAs substrates of  $n$ -type conductivity by the MOVPE. Post-growth technology of LED crystal formation includes a process of building in a metal reflector between the active area of the heterostructure and the substrate using operations of heterostructure transfer on the carrier substrate and removal of the growth substrate [7,8].

The need for selective removal of the growth substrate  $n$ -GaAs imposes certain requirements to the design and sequence of AlGaAs/GaAs-heterostructure layers growth. Epitaxial growth of the heterostructure starts with formation of a stop layer  $\text{Al}_{0.9}\text{Ga}_{0.1}\text{As}$  with high Al content, having high degree of etching selectivity towards the material of GaAs substrate in the compounds based on hydrogen peroxide and ammonia and on the basis of hydrogen peroxide and citric acid. Further a heavily-doped contact layer GaAs of  $n$ -type conductivity is crystallized, used to form an ohmic contact and also serving as a stop layer for selective removal of AlGaAs layer. Then a spreading layer  $\text{Al}_{0.2}\text{Ga}_{0.8}\text{As}$  of  $n$ -type conductivity is formed with thickness

increased to 4–6  $\mu\text{m}$ , since in this layer the textured light emitting surface is formed by etching method to depth of 1–2  $\mu\text{m}$ .

The active area of the heterostructure includes six InGaAs QWs, enclosed between  $\text{Al}_{0.2}\text{Ga}_{0.8}\text{As}$  layers and wide-band barrier  $\text{Al}_{0.4}\text{Ga}_{0.6}\text{As}$ -layers of  $n$ - and  $p$ -type conductivity. At the final stage of epitaxial growth, a highly doped contact layer GaAs is crystallized of  $p$ -type conductivity to form a rear point contact.

Technology of building in a metal reflector by transfer of a heterostructure onto a GaAs carrier substrate includes the following post-growth stages:

- formation of a point ohmic contact ( $\varnothing 10 \mu\text{m}$  with pitch of  $75 \mu\text{m}$ ) to a contact layer  $p^+\text{GaAs}$ ;
- removal of a contact layer  $p^+\text{GaAs}$  in areas free of a point ohmic contact;
- deposition of a metal reflector based on silver;
- installation of a GaAs carrier substrate using a gold–indium compound;
- removal of a growth substrate  $n\text{-GaAs}$  and a stop layer  $\text{Al}_{0.9}\text{Ga}_{0.1}\text{As}$ ;
- formation of a light emitting surface;
- deposition of a frontal ohmic contact to a contact layer  $n^+\text{GaAs}$ ;
- creation of a separating mesastructure  $1 \times 1 \text{ mm}^2$  and structure cutting;
- installation and packaging of LED crystals.

Formation of the light emitting surface of IR LEDs provides substantial impact on the emission extraction from the crystal and, accordingly, the optical capacity of the manufactured instruments. The main stages are:

- texturing of a light-emitting surface,
- deposition of a dielectric antireflection coating,
- installation of an optical element.

## 2. Texturing of light emitting surface

The technology of LED manufacturing uses various methods to texture the surface using plasma-chemical and liquid chemical etching [9,10]. Previous research [11] demonstrated that maximum values of electroluminescence were achieved when the light emitting surface was textured by liquid chemical etching method in two stages. Previously the contact layer  $n^+\text{GaAs}$  is etched in the dissolved etch based on hydrogen peroxide and ammonia ( $\text{NH}_4\text{OH}:\text{H}_2\text{O}_2$  at the weight parts ratio of 2:1) for 10 s, then the solid solution  $\text{Al}_{0.2}\text{Ga}_{0.8}\text{As}$  is textured in the etch based on fluoric acid, ammonium fluoride and hydrogen peroxide ( $\text{NH}_4\text{F}:\text{H}_2\text{O}_2:\text{HF}$  at the weight parts ratio 21:4:3) for 30 s. The profile of the textured surface measured on a stylus profiler is presented in Fig. 1, *a*, and the height of peaks was 1500–2500 Å. To form a more developed light emitting surface, the texturing was studied in the etch based on  $\text{NH}_4\text{F}:\text{H}_2\text{O}_2:\text{HF}$  for the solid solution  $\text{Al}_{0.2}\text{Ga}_{0.8}\text{As}$  together with the contact layer  $n^+\text{GaAs}$  for 30 s, without prior etching in ammonia-peroxide etch. Owing to the difference

in the etching speeds ( $V_{et}$ ) of semiconductor materials ( $V_{et,\text{GaAs}} < V_{et,\text{AlGaAs}}$ ),  $n^+\text{GaAs}$  layer performs the function of a local mask for etching  $\text{Al}_{0.2}\text{Ga}_{0.8}\text{As}$ . Therefore, height of the textured surface peaks increases to 3000–8000 Å (Fig. 1, *b*), which provides for the increase of the light emitting surface area and accordingly the maximum growth of electroluminescence intensity.

The light emitting surface as a result of texturing in the etch based on  $\text{NH}_4\text{F}:\text{H}_2\text{O}_2:\text{HF}$  for 30 s in the continuous etching mode has the appearance of hemispheres with smoothed frontal plane (Fig. 2, *a*), etching depth is 1–2  $\mu\text{m}$ . Therefore, when photons hit the smoothed area, no substantial change of the reflection angle will be observed, which will increase the loss of the emission share.

The mode of etching with interruption of the chemical reaction by intermediate flushing with deionized water was studied. Texturing was carried out in the etch based on  $\text{NH}_4\text{F}:\text{H}_2\text{O}_2:\text{HF}$  for the first three cycles of 10–12 s each with intermediate flushing. The etching depth remains, but at the same time the interruption of the chemical reaction causes suspension of the hemisphere formation process, and continued etching causes appearance of new hemispheres, which provides for formation of the developed textured surface with increased surface area to extract generated emission (Fig. 2, *b*).

The main difficulty of liquid chemical etching is achievement of the even wettability of the surface that affects homogeneity of etching. To analyze evenness of structure etching, distribution of LED crystal electroluminescence was recorded, using an optical microscope and a digital video camera, when the specified current is passed ( $I_{\text{LED}} = 10 \text{ mA}$ ). LED samples with heterogeneous texturing demonstrated appearance of spots that meant local reduction of electroluminescence intensity. Prior soaking of the surface with a flow of deionized water and mixing in process of etching makes it possible to achieve increased evenness of texturing and accordingly to increase the electroluminescence intensity.

## 3. Antireflection coatings

Additional increase of emission extraction from a LED crystal may be achieved by formation of antireflection coatings on the textured light extraction surface, providing for the reduction of the incident emission reflection coefficient and increased angle of the full inner reflection when coatings are used with the value of the refraction index between the semiconductor and air. To optimize the technology for formation of coatings with the minimum value of the reflection coefficient on the working wavelength of LEDs (850 nm), studies were completed for various materials to form single-layer and multiple-layer coatings: based on  $\text{TiO}_x$  (at  $x$  close to 2),  $\text{SiO}_2$ ,  $\text{Ta}_2\text{O}_5$ , applied by method of magnetron sputtering, and also based on  $\text{Si}_3\text{N}_4$ , deposited by the method of low-temperature plasma-activated pyrolysis.

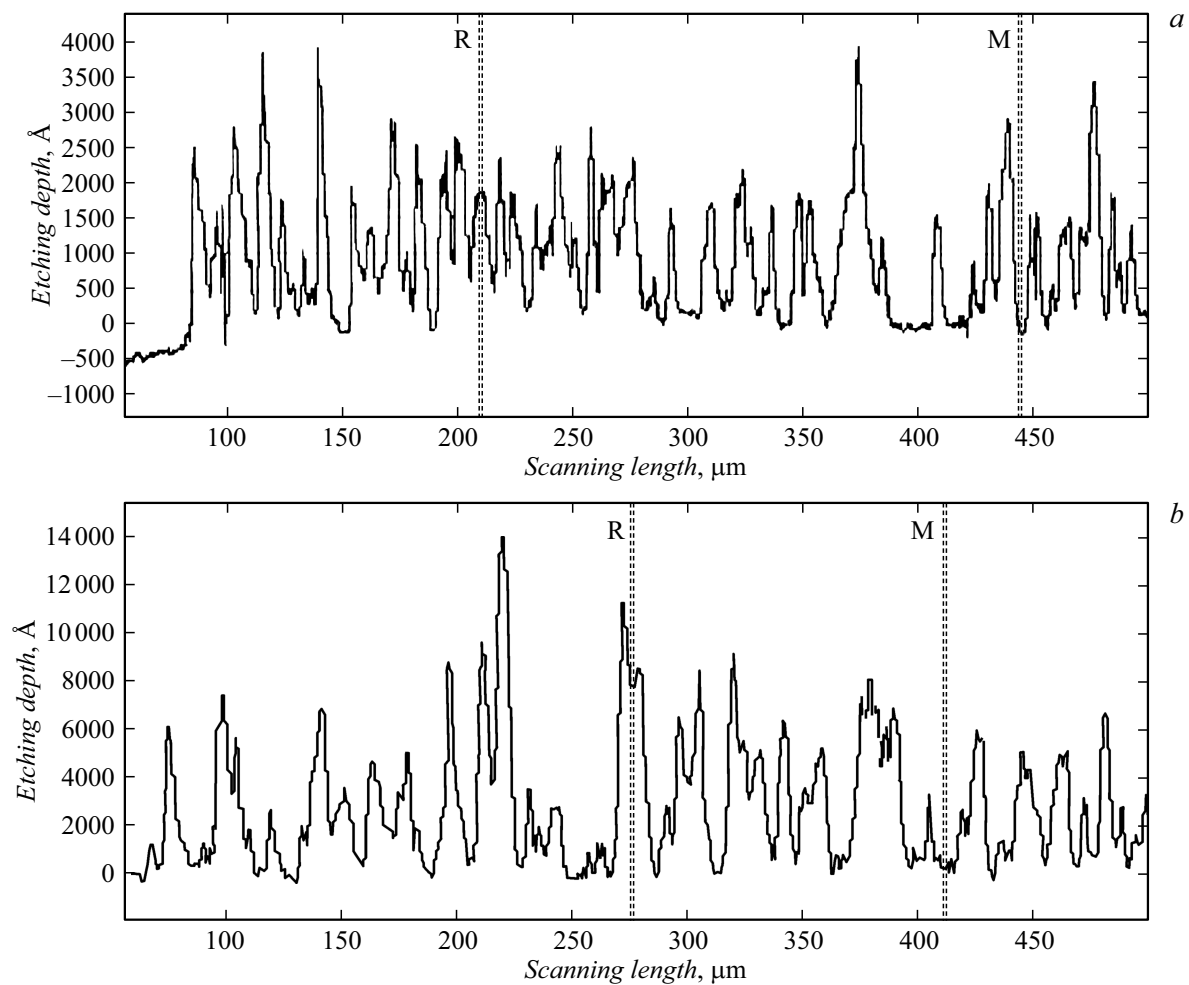


**Figure 1.** Profile of textured light emitting surface of LED at two-stage etching subsequently in etches  $\text{NH}_4\text{OH}:\text{H}_2\text{O}_2$  and  $\text{NH}_4\text{F}:\text{H}_2\text{O}_2:\text{HF}$  (a) and at one-stage etching in  $\text{NH}_4\text{F}:\text{H}_2\text{O}_2:\text{HF}$  (b).

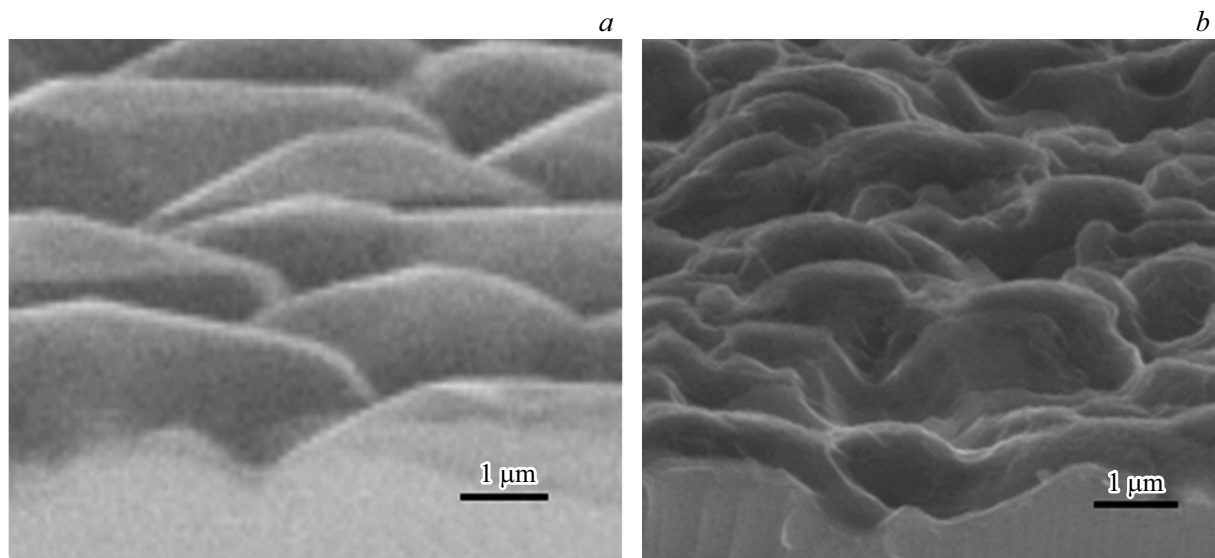


**Figure 2.** Image obtained on a scanning electron microscope for a cross section of AlGaAs/GaAs heterostructure after texturing of the surface in the etchant  $\text{NH}_4\text{F}:\text{H}_2\text{O}_2:\text{HF}$  in continuous mode (a) and in the mode with interruption of the chemical reaction (b).

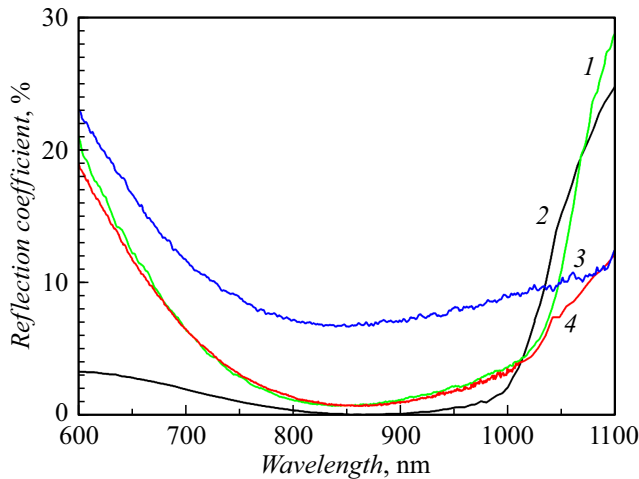


**Figure 3.** Spectral dependence of reflection coefficients of antireflection coatings based on  $\text{Si}_3\text{N}_4$  (1),  $\text{TiO}_x/\text{SiO}_2$  (2),  $\text{SiO}_2$  (3) and  $\text{Ta}_2\text{O}_5$  (4), applied on silicon substrate.

Studies of antireflection coating parameters were carried out by deposition of individual layers of the studied dielectric materials on the silicon substrate. The silicon substrate is selected for convenience of measurements in the wide range of wavelengths, since silicon absorbs emission with wavelength of up to 1000 nm. Distortion of the spectral dependence of the antireflection coatings reflection coefficient upon transition to the material of semiconductor heterostructure AlGaAs/GaAs is insignificant and was taken into account by recalculation of the thickness of deposited layers. For various antireflection coatings, spectral dependences of the normal emission reflection coefficient were measured on a spectroradiometer. During optimization of the thicknesses of layers and deposition parameters, minimum values were obtained for the reflection coefficient of emission from the silicon substrate with the applied antireflection coatings at wavelength 850 nm (Fig. 3). Studies demonstrated that the single-layer coating based on  $\text{SiO}_2$  does not provide low values of the reflection coefficient. Using a single-layer coating based on  $\text{Ta}_2\text{O}_5$  or  $\text{Si}_3\text{N}_4$  it is possible to reduce the reflection coefficient down to 0.5–1%. Deposition of the double-layer antireflection coating based on  $\text{TiO}_x/\text{SiO}_2$  provides for the reflection coefficient of  $< 0.1\%$  at wavelength 850 nm.

The important aspect in selection of the antireflection coating material is also the technology of its formation on the developed textured light emitting surface. The two-layer antireflection coating based on  $\text{TiO}_x/\text{SiO}_2$  is deposited by magnetron sputtering method. The feature of this method is material sputtering by a collimated beam, which positively impacts the homogeneity of the thickness of deposited layers on the smooth planar surface, but at the same time there is a considerable reduction of coating thickness on the inclined areas of the textured surface, which, in its turn, increases the reflection coefficient of the incident emission. The antireflection coating based on  $\text{Si}_3\text{N}_4$  is deposited by

the method of low-temperature plasma-activated pyrolysis, which provides for volumetrical even deposition of the coating both onto planar and developed surface.

Analysis of parameters of the manufactured LED crystals with application of the developed antireflection coatings ( $\text{TiO}_x/\text{SiO}_2$  and  $\text{Si}_3\text{N}_4$ ) demonstrated close values of optical capacity, which means the possibility to use such materials in process operations during instrument manufacturing.

#### 4. Optical element

Use of the optical element formed on the light emitting surface of the crystal substantially increases emission extraction from LED. OE is made after installation of the LED crystal onto the ceramic heat transfer base and bonding of current transfer golden wire.

Different OE types were studied: a silicon hemisphere and a plastic body with silicon fill (Fig. 4). OE was made by filling of two-component silicon of Elastosil® S604 brand with refraction index of  $\sim 1.34$  (at wavelength 850 nm) into a hemispherical matrix or in a plastic body. Further LED crystal was installed to OE, and silicon was polymerized. OE manufacturing in the form of a hemisphere facilitates emission extraction into the environment.

Technology of OE formation by silicon filling seals the LED crystal, which provides for its protection against the environmental parameters, making it possible to increase its service life, and reduces deterioration of photovoltaic parameters.

#### 5. IR LED parameters

IR LED parameters were determined in a pulse mode ( $\tau_{imp} = 5\text{--}300\ \mu\text{s}$ ), optical capacity was measured with account of spectral photosensitivity of a photodetector), and quantum efficiency was calculated using equation  $\eta_{ext} = \frac{P/(h\nu)}{I/e}$ , where  $P$  — measured optical power,  $P/h\nu$  — number of photons emitted by a light diode per second,  $I/e$  — number of injected electrons per second [6].

Measurements of the optical power (Fig. 5, a) and external quantum efficiency (EQE) (Fig. 5, b) were carried out for IR LEDs made using the above process methods:

- epitaxial growth of AlGaAs/GaAs-heterostructure with multiple QWs;
- building in a metal reflector based on silver that provides for the reflection coefficient of incident emission  $> 96\%$ ;
- transfer of  $n$ -GaAs heterostructure on a carrier substrate;
- growth substrate removal;
- even texturing of the light emitting surface by method of liquid chemical etching in the etch based on  $\text{NH}_4\text{F}:\text{H}_2\text{O}_2:\text{HF}$  in the mode with chemical reaction interruption;
- formation of the antireflection coating on the light emitting surface based on layers of  $\text{TiO}_x/\text{SiO}_2$ ;

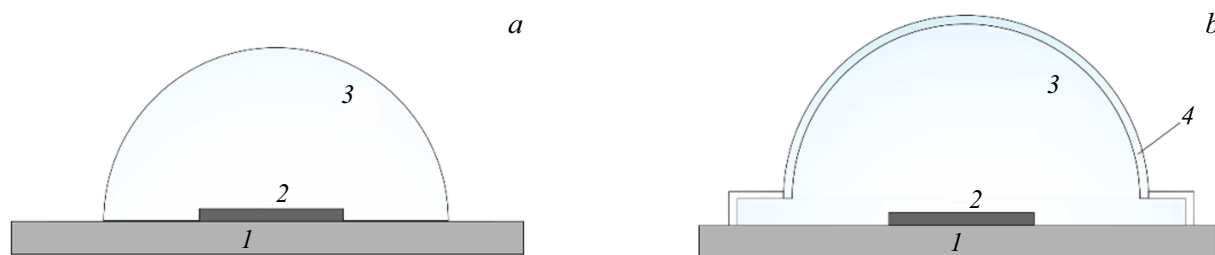


**Figure 4.** Schematic layouts of IR LEDs installed onto ceramic heat transfer bases, with a silicon hemisphere (a) and a plastic body (b): 1 — heat transfer base, 2 — LED crystal, 3 — silicon, 4 — plastic body.

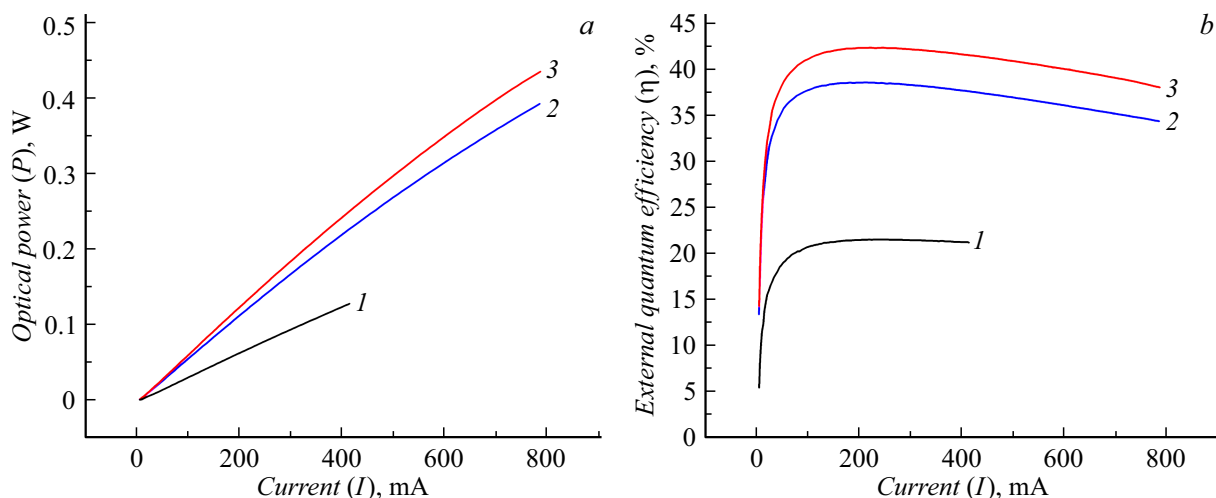


**Figure 5.** Dependence of optical capacity ( $P$ ) (a) and external quantum efficiency ( $\eta$ ) on current ( $I$ ) (b) of IR LED without OE (1), with OE from plastic body with silicon fill (2) and from silicon hemisphere (3).

— installation of OE of two types: a silicon hemisphere and a plastic body with silicon fill.

Use of various OE types provides significant impact on the optical power and external quantum efficiency of IR LEDs. Manufacturing of diodes without OE makes it possible to achieve values EQE  $\approx 22\%$  in the current range of 100–400 mA. Besides, OE installation causes approximately double EQE increase, which confirms substantial increase of emission extraction from the crystal. Optical power values  $> 400$  mW are achieved at current 800 mA. EQE  $\approx 42\%$  in the range of currents 150–300 mA are achieved using OE in the form of a silicon hemisphere. Optical power values and EQE of IR LEDs with OE made on the basis of the plastic body are slightly lower than when OE is used, which is made in the form of a silicon hemisphere, due to absorption of the emission share in the OE material. However, use of a plastic body substantially increases the device reliability, reduces the level of exposure to environmental parameters, increases the service life of LEDs.

In our previous research [12] the optical power values of 220 mW were achieved at current of 800 mA. Therefore, the completed developments made it possible to achieve the double increase of the optical power compared to previously published results.

## Conclusion

Research was carried out in the field of post-growth technology for IR LED manufacturing on the basis of epitaxial AlGaAs/GaAs-heterostructures aimed at increasing the emission extraction ( $\lambda = 850$  nm) and output optical power of devices. The method was developed for texturing of the light-emitting surface of LEDs with a compound based on  $\text{NH}_4\text{F}:\text{H}_2\text{O}_2:\text{HF}$  for three cycles of 10–12 s each with intermediate interruption of the chemical reaction. Antireflection coatings were optimized, the minimum reflection coefficient  $< 0.1\%$  was achieved for wavelength 850 nm when a double-layer coating is applied based on  $\text{TiO}_x/\text{SiO}_2$ . The technology is developed for formation of OE of two types: in the form of a plastic body with silicon fill providing for high reliability of the device operation and a silicon hemisphere making it possible to achieve the double increase of the optical power values ( $> 400$  mW at current of 800 mA).

## Conflict of interest

The authors declare that they have no conflict of interest.

## References

- [1] A.G. Entrop, A. Vasenev. *Energy Proced.*, **132**, 63 (2017). DOI: 10.1016/j.egypro.2017.09.636
- [2] M. Kitamura, T. Imada, S. Kako, Y. Arakawa. *Jpn. J. Appl. Phys.*, **43**, 2326 (2004). DOI: 10.1143/JJAP.43.2326
- [3] H.-J. Lee, L.-K. Kwac. *J. Luminescence*, **250**, 119086 (2022). DOI: 10.1016/j.jlumin/2022/119086
- [4] H.-J. Lee, G.-H. Park, J.-S. So, Ch.-H. Lee, J.-H. Kim, L.-K. Kwac, *Infrared Phys. Technol.*, **118**, 103879 (2021). DOI: 10.1016/j.infrared.2021.103879
- [5] H.-J. Lee, I.-K. Jang, D.-K. Kim, Y.-J. Cha, S.W. Cho. *Micromachines*, **13**, 695 (2022). DOI: 10.3390/mi13050695
- [6] E.F. Shubert. *Light-Emitting Diodes* (Rensselaer Polyt. Inst., NY, USA, 2018), ed. 3, p. 660.
- [7] A.V. Malevskaya, N.A. Kalyuzhnyy, D.A. Malevskii, S.A. Mintairov, A.M. Nadtochiy, M.V. Nakhimovich, F.Y. Soldatenkov, M.Z. Shvarts, V.M. Andreev. *FTP*, **55** (8), 699 (2021) (in Russian). DOI: 10.21883/FTP.2021.08.51143.9665
- [8] A.V. Malevskaya, N.A. Kalyuzhnyy, F.Y. Soldatenkov, R.V. Levin, R.A. Saliy, D.A. Malevskii, P.V. Pokrovskii, V.R. Larionov, V.M. Andreev. *ZhTF*, **93** (1), 170 (2023) (in Russian). DOI: 10.21883/JTF.2023.01.54078.166-22
- [9] Yuan Qin, Xia Guo, Wen Jing Jiang, Rong Fang, Guang Di Shen. *Proc. SPIE-OSA-IEEE Asia Communication and Photonics* (Shanghai, China, 2009), v. 7635, p. 763505-1.
- [10] R. Windisch, B. Dutta, M. Kuijk, A. Knobloch, S. Meinschmidt, S. Schoberth, P. Kiesel, G. Borghs, G.H. Döhler, P. Heremans. *IEEE Trans. Elect. Dev.*, **47** (7), 1492 (2000).
- [11] A.V. Malevskaya, N.D. Ilyinskaya, N.A. Kalyuzhnyy, D.A. Malevskii, Yu.M. Zadiranov, P.V. Pokrovsky, A.A. Blokhin, A.V. Andreeva. *FTP*, **55** (11), 1086 (in Russian). DOI: 10.21883/FTP/2021/11/51565/9679
- [12] A.V. Malevskaya, N.A. Kalyuzhnyy, D.A. Malevskii, P.V. Pokrovskii, V.M. Andreev. *ZhTF*, **94** (4), 632 (2024) (in Russian). DOI: 10.61011/JTF.2024.04.57534.261-23

*Translated by M.Verenikina*